Vysoká škola báňská - Technická univerzita Ostrava
Univerzitní studijní programy

Synthesis and characterization of powder nanocomposites of polypyrrole/phyllosilicate type

Syntéza a charakterizace práškových nanokompozitů typu polypyrrol/fylosilikát

Autor: Hana Koníčková

Vedoucí bakalářské práce: doc. Ing. Lenka Kulhánková, Ph.D.

Datum odevzdání: 16. 5. 2016

VŠB - Technical University of Ostrava
University Study Programmes
CNT - Nanotechnology Centre

Bachelor Thesis Assignment

Student:	**Hana Koníčková**
Study Programme:	B3942 Nanotechnology
Study Branch:	3942R001 Nanotechnology
Title:	Synthesis and characterization of powder nanocomposites of polypyrrole/phyllosilicate type Syntéza a charakterizace práškových nanokompozitů typu polypyrrol/fylosilikát
The thesis language:	English

Description:

During the processing of a bachelor's thesis the student acquires theoretical and practical knowledge about the preparation technology of composite materials of conductive polymer/phyllosilicate type. Following part of the work will be focused on processing of composite materials into pressed tablets and their characterization by measuring the electrical conductivity using direct current. In the third part of this work the structure characterization of prepared samples using XRD analysis will be performed. Experimentally obtained values of the interlayer distances will be compared with simulated diffraction patterns calculated from atomistic models prepared by student. Geometry optimization of these models will help to clarify the inner structure of prepared composites.

1. Find and read literature on a given topic.
2. Preparation of powdered nanocomposites of polypyrrole/montmorillonite type.
3. Structure characterization of the prepared samples.
4. Familiarize with modeling environment of Materials Studio.
5. Preparation and geometry optimization of atomistic models of polypyrrole/montmorillonite nanocomposites.
6. Comparison of experimental and calculated data and description of the inner structure of nanocomposite.

References:

Z. Weiss, M. Kužvart: Jílové minerály, Univerzita Karlova v Praze, nakladatelství Karolinum, 2005.

Lerf A., Čapková, P.: Encyclopedia of nanoscience and nanotechnology. American Scientific publishers, Stevenson Ranch, California, USA (2003), 1-54.

Mravčáková M., Omastová M., Olejníková K., Pukánszky B., Chehimi M.M.:The preparation and properties of sodium and organomodified- montmorillonite/polypyrrole composites: A comparative study. Synthetic Metals 157 (2007) 347-357.

Comba P., Hambley T.W.: Molecular Modeling of Inorganic Compounds. Weinheim, New York, Basel, Cambridge, Tokyo, VCH, 1995.

Rappé A. K, Casewit C. J, Colwell K. S, Goddard W. A., Skiff W. M.: UFF a full periodic table force field for molecular mechanics and molecular dynamics simulations. Journal of the American Chemical Society 114 (1992) 10024-10035.

Extent and terms of a thesis are specified in directions for its elaboration that are opened to the public on the web sites of the faculty.

Supervisor: **doc. Ing. Lenka Kulhánková, Ph.D.**

Consultant: Ing. Jonáš Tokarský, Ph.D.

Date of issue: 20.10.2015

Date of submission: 16.05.2016

prof. Ing. Jaromír Pištora, CSc.
Head of Department

prof. Ing. Petr Noskievič, CSc.
Vice-rector for Study Affairs

Prohlašuji, že jsem celou bakalářskou práci včetně příloh vypracovala samostatně pod vedením vedoucího bakalářské práce a uvedla jsem všechny použité podklady a literaturu. Byla jsem seznámena s tím, že na moji bakalářskou práci se plně vztahuje zákon č. 121/2000 Sb. – autorský zákon, zejména §35 – užití díla v rámci občanských a náboženských obřadů, v rámci školních představení a užití díla školního a §60 – školní dílo. Beru na vědomí, že Vysoká škola báňská – Technická univerzita Ostrava (dále jen VŠB-TUO) má právo nevýdělečně ke své vnitřní potřebě bakalářskou práci užít (§35 odst. 3). Souhlasím s tím, že jeden výtisk bakalářské práce bude uložen v Ústřední knihovně VŠB-TUO k prezenčnímu nahlédnutí a jeden výtisk bude uložen u vedoucího bakalářské práce. Souhlasím s tím, že údaje o bakalářské práci, obsažené v Záznamu o závěrečné práci, umístěném v příloze mé bakalářské práce, budou zveřejněny v informačním systému VŠB-TUO. Bylo sjednáno, že s VŠB-TUO, v případě zájmu z její strany, uzavřu licenční smlouvu s oprávněním užít dílo v rozsahu §12 odst. 4 autorského zákona. Bylo sjednáno, že užít své dílo – bakalářskou práci nebo poskytnout licenci k jejímu využití mohu jen se souhlasem VŠB-TUO, která je oprávněna v takovém případě ode mne požadovat přiměřený příspěvek na úhradu nákladů, které byly VŠB-TUO na vytvoření díla vynaloženy (až do jejich skutečné výše). Beru na vědomí, že odevzdáním své práce souhlasím se zveřejněním své práce podle zákona č. 111/1998 Sb., o vysokých školách a o změně a doplnění dalších zákonů (zákon o vysokých školách), ve znění pozdějších předpisů, bez ohledu na výsledek její obhajoby.

V Ostravě: 16. 5. 2016

Hana Koníčková

K Vodárně 135, 742 83 Zbyslavice

Prohlašuji:

Prohlašuji, že svou bakalářskou práci na téma: "Synthesis and characterization of powder nanocomposites of polypyrrole/phyllosilicate type", jsem vypracovala samostatně s použitím doporučené literatury. Tímto dávám souhlas k jejímu dalšímu využití.

V Ostravě: 16. 5. 2016 Podpis:.....

Anotace

Tato práce je zaměřena na přípravu a charakterizaci práškových nanokompozitů typu polypyrrol/fylosilikát. Vodivé nanokompozity byly připraveny jednokrokovou metodou, při které současně proběhla interkalace a polymerace pyrrolu v přítomnosti montmorillonitu s využitím dvou různých oxidačních činidel – chloridu železitého a peroxodisíranu amonného. Připravené nanokompozity byly analyzovány pomocí skenovací elektronové mikroskopie, rentgenové difrakční analýzy, infračervené spektroskopie, Ramanovy spektroskopie a termogravimetrické analýzy. Pomocí molekulárního modelování byla vytvořena série modelů, které byly optimalizovány a porovnány s výsledky z termogravimetrické analýzy a rentgenové difrakční analýzy. Vyhodnocením připravených modelů bylo získáno možné vnitřní uspořádání připravených nanokompozitů polypyrrol/montmorillonit.

Klíčová slova: polypyrrol, montmorillonit, nanokompozity, molekulární modelování.

KONÍČKOVÁ, Hana. *Synthesis and characterization of powder nanocomposites of polypyrrole/phyllosilicate type*. Ostrava, 2016. Bakalářská práce. Vysoká škola báňská - Technická univerzita Ostrava. Vedoucí práce Doc. Ing. Lenka Kulhánková, Ph.D., 45s.

Annotation

This work is focused on the preparation and characterization of powder nanocomposites of polypyrrole/phyllosilicate type. Conducting nanocomposites were prepared by one–step method in which simultaneously intercalation and polymerization of pyrrole in the presence of montmorillonite using two different oxidants – ferric chloride and ammonium peroxydisulfate – took place. Prepared nanocomposites were analysed using scanning electron microscopy, X–ray diffraction, infrared spectroscopy, Raman spectroscopy, and thermogravimetric analysis. With molecular modeling was created a series of models that were optimized and compared with the results of thermogravimetric analysis and X–ray diffraction analysis. By evaluation of prepared models were obtained possible internal arrangements of prepared nanocomposites of polypyrrole/montmorillonite type.

Keywords: polypyrrole, montmorillonite, nanocomposites, molecular modeling.

KONÍČKOVÁ, Hana. *Synthesis and characterization of powder nanocomposites of polypyrrole/phyllosilicate type*. Ostrava, 2016. Bachelor thesis. VŠB – Technical University of Ostrava. Supervisor Assoc. Prof. Ing. Lenka Kulhánková, Ph.D., 45s

Content

1. Introduction

This work is focused on the preparation and characterization of powdered nanocomposites based on polypyrrole/phyllosilicate. Literature review of conducting polymer – polypyrrole, layered silicates nanocomposites, and molecular modeling was the very first step. In the next step, a one–step method was used for preparation of nanocomposites, with various content of polypyrrole, which were subsequently analyzed by a number of instrumental techniques (Scanning electron microscopy, Fourier transform infrared spectroscopy, Raman spectroscopy, thermogravimetric analysis, and X–ray diffraction). Then I have become acquainted with Materials Studio modeling environment, in which I build atomistic models, which were then optimized, therefore, to select such models (according to similarities with the available experimental data) that are the closest to reality. There is no such experimental technique that would allow us to look inside the interlayer space (direct look at it, its structure). In the end I was able, through comparison of experimental and calculated data, to clarify the internal arrangement of the prepared nanocomposites.

2. Theoretical part

2.1 Conducting polymers

Polymers are long chains consisting of repeated constitutional unit. Common polymers (for example polyethylene or polyvinylchloride) are not electrically conductive and are used as great electric insulants. However, there is a group of polymers which are conductive. Conducting polymers (for example polyacetylene, polypyrrole or polyaniline) show, unlike the other polymers, their own electrical conductivity. They consist of a system of conjugated double bonds which, together with the presence of charge carriers, are prerequisites for electrical conductivity [1].

2.1.1 Polypyrrole

In recent past, conducting polymers have been studied as advanced materials. Polypyrrole (PPy), as one of representatives of the conducting polymers, is chanceful for commercial applications, because it has great environmental stability, easy preparation and higher electrical conductivity than other conducting polymers. Oligomer products were obtained by chemical oxidation of pyrrole in 1887. The information that pyrrole polymerizes in acidic environment by oxidation with hydrogen peroxide to form an insoluble pyrrole black was published in 1916. Pratesi [3] shows the composition of PPy $C_{4.00–4.5}$ $H_{3.0–4.5}$ $N_{1.0}$ $O_{1.0–1.5}$. It is obvious that the structure shown in Fig. 1 is idealized, without the presence of oxygen [2].

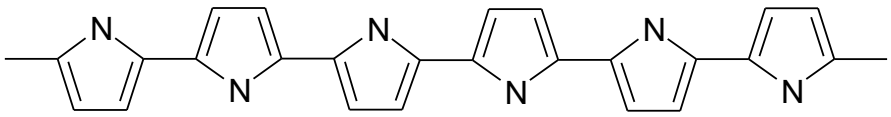

Fig. 1 *Polypyrrole chain.*

2.1.2 Properties of polypyrrole

Chemical oxidation of pyrrole leads to a black powder – pyrrole black. Many of PPy properties are studied on electrochemically prepared PPy thin films. There is also an influence of used precursors (dopant, solvent – in electrochemical polymerization), for its impact to electrical conductivity. The stability in the air is comparatively high – their degradation happens only above 150 – 300 °C (according to the dopant anion). The thermal degradation of PPy begins with the decrease or decomposition of dopant. Another deprotonation (or next decrease of dopant) at higher temperatures is always accompanied by a formation of structures of imine shape in the polymer [4].

The PPy is amorphous and generally gives just a diffuse halo in X–ray diffraction patterns. The electron diffraction revealed that there are up to 15% (of whole volume) of crystalline domains in the bulk of amorphous PPy. The experimental data shows

that the crystalline regions have a monoclinic lattice. That means that the pyrrole rings in the chain are oriented (according to nitrogens) in opposite directions (Fig. 2) [4].

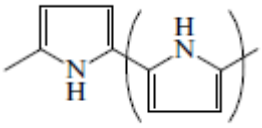

Fig. 2 *Orientation of pyrrole rings [4].*

The obtained data from infrared spectroscopy and nuclear magnetoresistance analysis of the products of oxidative decomposition of PPy demonstrate that pyrrole rings are connected in α–α′ positions. This conclusion is confirmed by the fact that α–substituted pyrrole derivatives do not polymerise upon oxidation. The theoretical calculations indicate that a certain amount of bonds is formed in β – positions [4].

The PPy chains are planar and are ordered in layers parallel to the film surface (the distance between plains is 0.341 nm). The PPy chains, which are in the plain, are not oriented. The anions of the dopant intercalate the interplanar space between the PPy chains. The X–ray photoelectron spectroscopy revealed that electrostatic interactions between oxidised PPy chains and dopant anions (ClO_4^-, polyvinylsulfonate) happen through the π–system of the rings rather than through heteroatoms of the rings. According to the data from electron diffraction could be said that polymer chains are ordered. The fast charge transfer along the polymer chains and the rapid exchange between the macromolecules are related with studies of conductivity which also indicates that polymer chains are to a certain extent ordered. The degree of polymer ordering significantly influences its conductivity. X–ray diffraction showed that a presence of multi–charged anions in the process of preparation of the PPy films has a different effect on the regularity of the film (films are more ordered) than a presence of single–charged anions [4].

PPy is insoluble in organic solvents which is a difficult problem for measuring its molecular mass [4].

The mechanism of charge transport is a special subject of interest in PPy conduction. The charge carriers are polarons and bipolarons and they are formed upon doping. Chemically, the formation of a polaron is equal to formation of a radical cation (Fig. 3) and formation of a bipolaron is equal to formation of a dication (Fig. 4) [4].

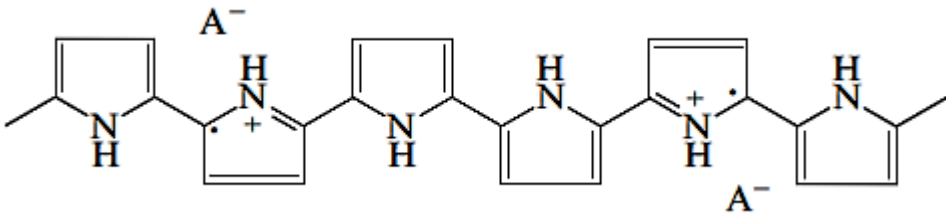

Fig. 3 *Polaron [4].*

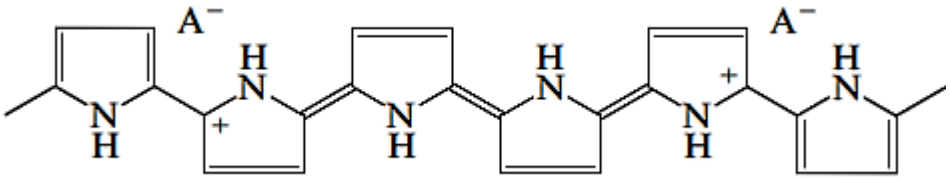

Fig. 4 *Bipolaron [4].*

The polaron and bipolaron are extended structures that are spread over three to four monomer units of the chain [4].

The specific interest is put on interchain interactions and charge transfer. The dopant, used in synthesis, compensates the charge of free charge carriers and also magnifies the probability of interchain charge transfer because of a large overlap of dopant's atomic orbitals with the π–orbitals of the atoms of carbon. The conductivity along the surface is generally higher that perpendicular because the polymer chains are primarily orientated parallel to the film surface. There also exist records that the conductivity increases with decreasing temperature (which is a behaviour proper to metals). The conditions of polymers' synthesis heavily affect their conductivity. Significant changes in conductivity usually appear in the earlier phases of doping and its additional increase is inconsequential [4].

The conductivity of PPy films shifts by several decimal orders which depends on the used anion in the synthesis. In most cases the conductivity is higher for anions that have lower nucleophilicity. The storage of PPy films in air leads to a decrease of their conductivity (conductivity of films with large organic anions is reduced slowly) [4].

2.1.3 Synthesis of polypyrrole

Part of development of conducting polymers held after 1979 when an electrochemical preparation of PPy was published. PPy was electrochemically prepared from monomer solution in acetonitrile or propylene carbonate with low water content in the presence of dopant (for example tetramethylammonium tetrafluoroborate). On platinum electrode was created a film, which conductivity reached up to 100 $S \cdot cm^{-1}$ [2].

In 1982 were published works describing electrochemical synthesis of PPy in aqueous solutions. Mechanism of electrochemical polymerization of pyrrole isn't yet fully understood. It is assumed that in the first step a pyrrole radical cation is created which then reacts with another cation radical to form a dimer while eliminating two protons. Propagation of the chain proceeds like a recombination of a radical dimer with other cation radicals for simultaneous deprotonation [2].

Chemical polymerization of pyrrole is better than electrochemical polymerization to obtain a bigger amount of PPy. Nowadays, many laboratories are working on improvement of the process of chemical preparation of PPy in order to obtain a product with high conductivity. In chemical polymerization of pyrrole is possible to use a variety of oxidizing agents – for example ammonium peroxydisulfate, hydrogen peroxide and different kind of salts containing ions of transition metals (for example Fe^{+3}, Cu^{2+}, Cr^{6+}, Ce^{4+}, Ru^{3+}, and Mn^{7+}). In practice is preferred ferric chloride due to higher conductivity of prepared PPy [2].

2.1.4 Utilization of polypyrrole

The results of the first electrochemical studies of PPy led to conclusion that PPy is stable enough and can be used as a non–metal material for electrodes [4].

It is also a chanceful material for rechargeable lithium batteries because of the great advantages of the polymer electrodes such as low weight combined with high energy storage capacity and an opportunity to produce and use them as thin films [4].

The conducting polymers' conductivity is tender to chemical reagents which grant a possibility of development of different sensors based on them. PPy can be used as a sensor for specific constituents in gas mixtures, including both organic (acetone, ethanol, methanol) and inorganic (NO, CO_2, NH_3, H_2S) constituents. The PPy–based amperometric biosensors with included enzymes like alcohol dehydrogenase, peroxidase, glutamate oxidase and glucose oxidase may find large applications [4].

The biocompatibility and non–toxicity of PPy allows, by electrochemical reduction of oxidative doped polymer, to controllably deliver an organism (cell) with microscopic doses of an immobilised drug in ionic form. PPy can be applied in biological media as an effective conductor (for example to regenerate a nerve tissue) [4].

One of auspicious subject is the application of PPy in form of a protective coating for semiconducting anodes in photoelectrochemical cells. The semiconductor covered in PPy film will not oxidise like in the photochemical reaction when uncovered (semiconductors are placed in humid media where the reaction takes place which leads to the oxidation and the electrodes become useless). The polymer cover prevents passivation of electrode surface and currently allows formation of electron holes which go over to the polymer (the reaction takes place on polymer's surface). Flexible PPy films can be used as protective electromagnetic shields. Electrochemically deposited PPy films on a surface of porous silicone were used in structure of an electroluminescent diode as electric contacts [4].

2.2 Phyllosilicates

Silicates are the most important group of minerals in Earth's crust. They usually occur like small particles of lamellar or rail–like shape with size about few micrometres. They can also appear in bigger sizes in hydrothermal and metamorphic environment like crystals reaching centimetres or even larger [6]. Silicates can be divided into five

groups: sorosilicates, cyclosilicates, inosilicates, phyllosilicates (clay minerals), and tectosilicates [5].

2.2.1 Structure and properties

Layered silicates (also called phyllosilicates or planar silicates) are classified based on the structural and chemical properties of its structural unite. A structural characteristic is a type of silicate layer. Chemical characteristics are size of charge on the layers and character of the material in the space between layers [5].

Main building element of layered structure of phyllosilicates are nets of tetrahedrons $[TO_4]^-$ and octahedrons $[MA_6]^-$ [5].

Tetrahedral net is created by connection of peaks of the basal oxygen atoms (O_b) of tetrahedrons. The fourth atom of oxygen, indicated as apical (O_a), heads to random side which is vertical to plain of tetrahedral network (Fig. 5a). The tetrahedral network (T) has in ideal case a hexagonal symmetry (Fig. 5b). The height of tetrahedral network means a distance between the average value of vertical coordinates of the basal oxygens and apical oxygens [5].

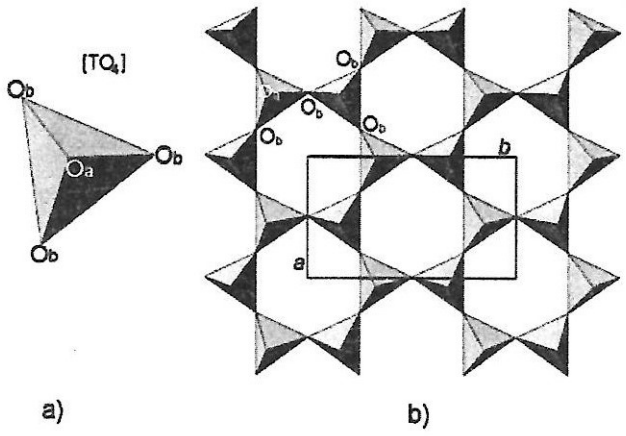

Fig. 5 *Tetrahedron and tetrahedral network: a) Tetrahedron $[TO_4]^-$, b) Tetrahedral network with apical (O_a) and basal (O_b) atoms of oxygen. Main orthogonal cell T_4O_{10} is marked by vectors **a** and **b** [5].*

In tetrahedral networks of phyllosilicates occur tetrahedrons $[SiO_4]^{4-}$, $[AlO_4]^{5-}$ or $[FeO_4]^{5-}$. The isomorphic substitution (Si^{4+} cations in tetrahedrons by Al^{3+} or Fe^{3+} cations) is not accidental, but exists in domains. The change of the charge of layer depends on substitutions Si^{4+} cations in tetrahedrons. Chemical composition of tetrahedral network is usually defined by main orthogonal cell (general formula T_4O_{10}) or main hexagonal cell (T_2O_5) [5].

Octahedral network (Fig. 6b) is made of two tightly arranged planes of O^{2-} and OH^- anions. Central cation positions in octahedrons (M) are most often occupied by Al^{3+}, Fe^{3+}, Fe^{2+}, Mg^{2+} cations, less often with Li^+, Mn^{2+}, Co^{2+}, Ni^{2+}, Cu^{2+}, Zn^{2+}, V^{3+}, Cr^{3+}, and Ti^{4+} cations. Octahedrons $[MA_6]^-$ are connected to each other by edges and peaks. The height of octahedral network is determined by the distance of the lower and the upper plane of anions (A). The anions (OH^-, F^-, Cl^-, O^{2-}) in octahedral network have the orientation *cis* or *trans* (Fig. 6a) [5].

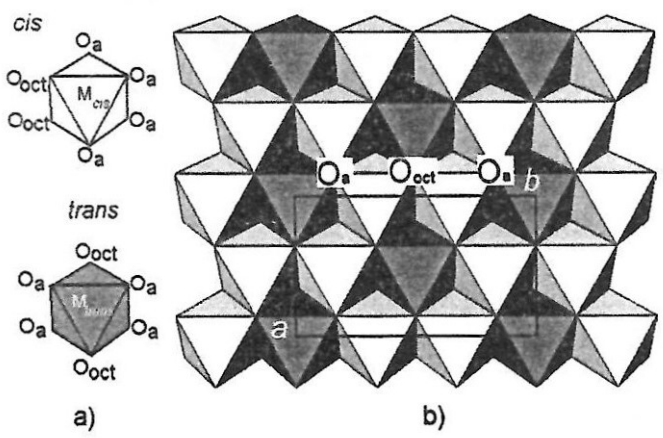

Fig. 6 *Octahedrons and octahedral network: a) Octahedrons with occupation O_{oct} (OH^-, F^-, Cl^-, O^{2-}) in positions cis and trans, b) Octahedral network with distribution of positions of anions cis and trans. Apical (O_a) atoms of oxygen and shared octahedral anoint [5].*

The smallest structural unit of octahedral network are three octahedral positions (Fig. **7**). Trioctahedral phyllosilicates have all three positions occupied by cations (Fig. **7**a). Dioctahedral phyllosilicates have only two of three positions occupied by cations, the third position is vacant (Fig. 7b) [5].

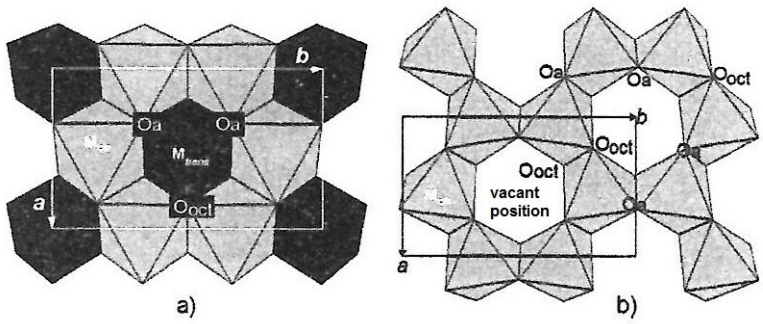

Fig. 7 *Octahedral networks: a) Trioctahedral, b) Dioctahedral. Apical oxygens of octahedrons O_a, positions of anions O_{oct} between adjoining octahedrons and vacant positions. Vectors* ***a*** *and* ***b*** *of main orthogonal cell [5].*

There are two types of layered structure of phyllosilicates. The first one is layered structure 1:1 (Fig. 8). Octahedral and tetrahedral network are mutually connected by means of apical oxygen atoms [5].

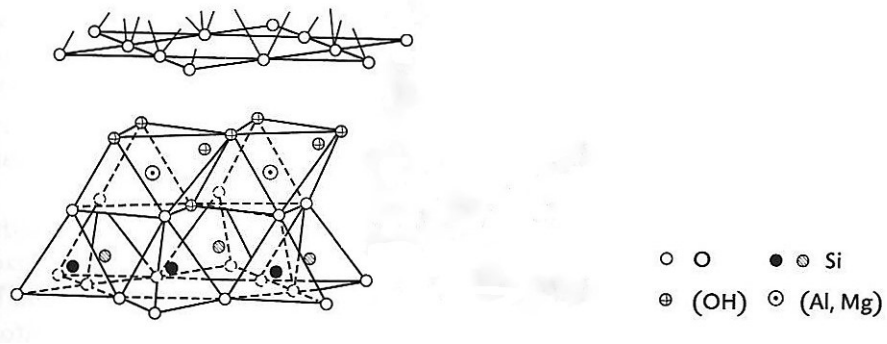

Fig. 8 *Layered structure 1:1 [6].*

The surface of 1:1 layers on the side of tetrahedrons is formed by basal atoms of oxygen of tetrahedral network – *siloxane surface* – and the surface on the side of octahedrons is formed by hydroxyl OH^- groups of octahedral network – *hydroxide, aluminol surface*. The composition of 1:1 layers can be expressed within one main structural unit by the general crystallochemical formula. The orthogonal cell consists of six octahedrons (M) and four tetrahedrons (T) and then the formula can be interpreted like:

$$T_4M_6O_{10}(OH)_8$$

The second one is layered structure 2:1 (Fig. 9). It represents the connection of two tetrahedral networks, with opposite polarity, with one octahedral network that is in between them. The unshared atoms of oxygen in tetrahedrons create two planes of basal oxygens on both surfaces.

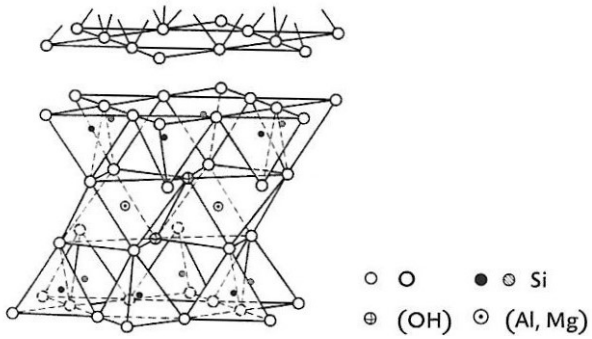

Fig. 9 *Layered structure 2:1 [6].*

The orthogonal cell comprises of six octahedrons and eight tetrahedrons and the general formula can be expressed like:

$$T_8M_6O_{20}(OH)_4$$

Basic structural unit was defined like a layer plus interlayer space. The interlayer material is defined like a substance between two plains of basal atoms of oxygen across the interlayer space [5].

2.2.2 Montmorillonite

Montmorillonite (MMT) belongs to smectite clays. They are ordered in 2:1 composition which means that the layer is formed from two networks of tetrahedrons and one network of octahedrons between them. Octahedral network is created by two layers of closely arranged anions O^{2-} and OH^-. Central cation position is mostly filled with cations Al^{3+}, Fe^{3+}, Fe^{2+}, Mg^{2+}, less often with Li^+, Mn^{2+}, Co^{2+}, Ni^{2+}, Cu^{2+}, Zn^{2+}, V^{3+}, Cr^{3+} and Ti^{4+}. Networks of tetrahedrons and network of octahedrons are connected like is shown in Fig. 10 [5].

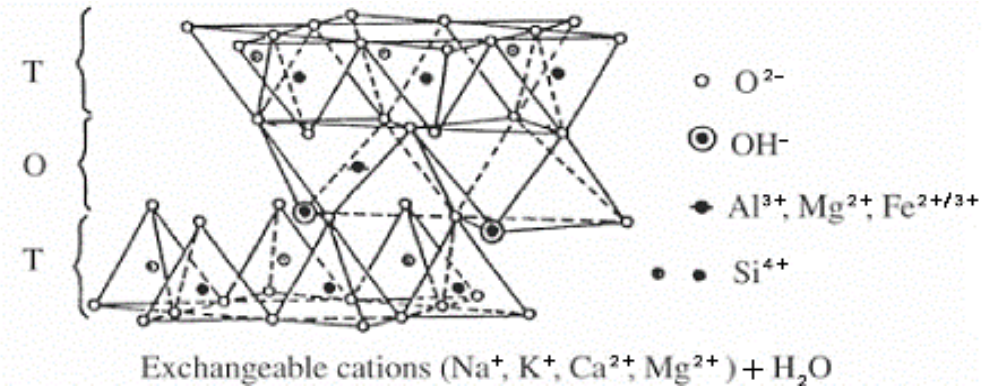

Fig. 10 *Montmorillonite structure. T: tetrahedral sheet, O: octahedral sheet [7].*

The structure is expandable, has a negative charge on the layers (0.2 – 0.6 el.) and contains hydrated exchangeable cations in interlayer space. The charge on the layers is mainly caused by substitution Mg^{2+} by Al^{3+} in octahedrons. Crystallochemical formula of idealized structure of montmorillonite can be for example $Si_4(Al_{1.5}Mg_{0.5})O_{10}(OH)_2$. Different types of montmorillonite were classified according to the location of their occurrence [5].

2.2.3 Composite materials

Nanocomposites can be divided in three types according to dimensions that are in nanoscale. When all of three dimensions are in nanoscale (<100 nm), we deal with isodimensional nanoparticles (spherical silica nanoparticles, semiconductor nanoclusters). When two dimensions are in the order of nanometers and the third is not (is much larger and forms an extended structure) we speak about nanotubes or whisker (carbon nanotubes, cellulose whiskers) that are the subject of extensive research as reinforcing nanofillers providing materials with extraordinary properties. The third type of nanocomposites has only one dimension in nanoscale. The filler is presented in the form of sheet with thickness of a few nanometers and hundreds to thousands nanometers long. This group of composites can be summarized as polymer/layered crystal nanocomposites. These materials are nearly solely obtained by the intercalation of the polymer (or a monomer that is as follows polymerized) into the galleries of layered host crystals. Wide range of both synthetic and natural crystalline fillers is under specific conditions

able to intercalate a polymer. The precursors base on layered and clay silicates are, among all the potential, a greater extent investigated due to the high and easy availability clay materials and because their intercalation chemistry has been studied for a long time [8].

Nanocomposites of polymer/phyllosilicate type are new type of materials. They are usually based on smectite clays and are usually hydrophobic because of ionic exchange of the sodium interlayer cation with an onium cation. The nanocomposites can be prepared through various methods of synthesis containing exfoliation, adsorption, in situ intercalative polymerization and melt intercalation. There are two types of structure that can be obtained. The first are intercalated nanocomposites, where polymer chains are placed between silicate layers, and the second are exfoliated nanocomposites which have individually separated silicate layers that are more or less equally dispersed in the polymer matrix. This new group of materials demonstrates superior properties, at very low filler level (around 5 wt.%), such as the increase in thermal stability and gas barrier properties; enhancement of Young's modulus and storage modulus; good flame retardancy [8].

2.2.4 Intercalation of phyllosilicates

There are three types of composites that are obtainable when phyllosilicate is associated with a polymer. It depends on the character of the components used (phyllosilicate, organic cation and polymer matrix) and the method of synthesis [8].

The phase separated composite is gained when the polymer is not able to intercalate between the phyllosilicate layers (Fig. 11a). This composite has the same properties as microcomposites. Intercalated structure (Fig. 11b) which has one or more extended polymer chains intercalated between the phyllosilicate sheets which results into a well ordered multilayer morphology constructed form alternating polymer and inorganic layers. The third and last type is exfoliated or delaminated structure (Fig. 11c). The phyllosilicate layers are completely separated and scattered in the polymer matrix. The intercalation of the polymer chains usually increase the interlayer spacing which can be detected by X–ray diffraction (compared with original clay there is a shift of the diffraction peak). For characterizing the composite's morphology is used transmission electron spectroscopy [8].

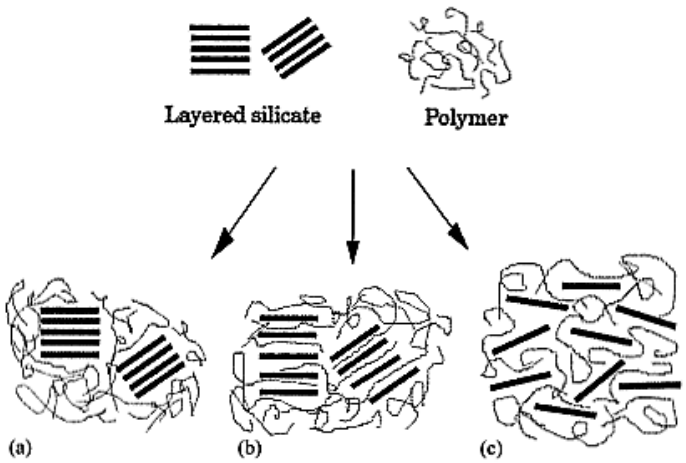

Fig. 11 *Different types of composites formed after interaction of layered silicates and polymers: a) Phase–separated microcomposite; b) Intercalated nanocomposite; c) Exfoliated nanocomposite [8].*

Through the techniques that are used for nanocomposite preparation there are four main processes: exfoliation–adsorption, *in situ* intercalative polymerization, melt intercalation, template synthesis [8].

The *in situ* intercalative polymerization is described because its utilization in this thesis. The description of the other methods is available in article cited. The layered silicate swells in liquid monomer (or its solution) so that polymer formation can take place between intercalated layers. Polymerization may be initiated either by heat, radiation or diffusion of a suitable organic initiator or catalyst docked through cation exchange within the interlayer before swelling of monomer [8].

The interlayers of Na^+ MMT are filled with sodium cations which improve the hydrophilic properties and leads to a high degree of swelling in water. In case of used aqueous systems for intercalation procedure, these effects therefore provide an effective method for the preparation of intercalated nanocomposites [9].

2.2.5 Composites with polypyrrole

In the course of time, polymer/layered silicate nanocomposites have drawn significant attraction for several engineering applications (enhanced mechanical property and thermal stability, reduced gas permeability, self–extinguishing flame retardant

characteristics). The connection of conducting polymer and phyllosilicate in nanocomposites provides the new synergistic properties that cannot be obtained from individual materials. For example, more easily controlled conductivity and the improvement of mechanical or thermal stability which provides the synthesis of the nanocomposites [9].

The PPy/Na^+ MMT nanocomposite can be prepared through an inverted emulsion pathway polymerization. The nanocomposite particles synthesized by this method where examined by various methods to characterize their physical and chemical properties. The intercalation of PPy into the galleries of MMT was observed from the X–ray diffraction and Fourier transform infrared spectroscopy patterns (characteristic peaks of PPy). The conductivity of nanocomposite was lower than of the pure PPy in a board range of temperature because clay effects as an insulating material [9].

2.3 Molecular modeling

The molecular modeling can be divided into two different parts. First part is molecular mechanics and the second one is quantum mechanics [10]. Only molecular mechanics was used in this work and will be described below.

Chemists imagine molecules from the perspective of bond lengths, bond angles and dihedral angles. All this information is also included in the set of Cartesian coordinates for the constituent atoms (molecule containing N atoms has 3N Cartesian coordinates). Scientists who deal with spectroscopy, are generally interested in finding a collection of equilibrium, geometric parameters and force constants that fits perfectly with their experimental data. They want a *force field* (containing equilibrium quantities, force constants and every other comprised parameter) that is particular for a given molecule. They want their incredibly precise measurements to agree with theory. If the force field contains only chemical terms (like bond lengths, bond angles and dihedral angles) it is denoted as a *valence force field*. Molecular modelers want a force field that can be transferred from molecule to molecule (for example to predict the geometry of a new molecule using data they get from other kindred molecules). They make use of the bond concept referring to traditional ideas that a molecule is a number of bonded atoms and a large molecule consists of the same properties like small molecules but combined in different ways [10].

The name *molecular mechanics* was created in 1970s as a description of the application of classical mechanics to determinate the molecular equilibrium structures. In molecular mechanics we consider non–bonded interactions and of course the chemical meaning of each atom (for example sp carbon atom is different from an sp^2 carbon) The idea is to use the force field as ensemble of constants that are supposed to be fixed by referring to experiment or stricter calculation. *Urey–Bradley force field* is a valence force field containing non–bonded interactions [10].

A new force field – *Universal force field* was developed in order to deal with studies of variety of atomic associations – organic molecules or metal compounds (in this case, really complicated structure of MMT with substitutions and organic compound – PPy). It uses general rules for estimation of force field parameters based on simple relations. The set of basic parameters is based just on the element, its connectivity, and hybridization [11].

The search for minima on the molecular potential energy surface of large molecules is a problem that a molecular mechanics tend to be concerned about. This problem is denoted as an *optimization theory* and it, now as a part of applied mathematics, employs many mathematicians, scientists and engineers with its related problems. The first "by hand" calculations for the molecular mechanics optimization were made by F. H. Westheimer in 1956. J. B. Hendrickson was the first one who has done the computer calculations. Actually their methods were not suitable and applicable for molecules. Over the years, many algorithms have been developed (some of them appropriate for molecular mechanics, some for quantum mechanics). In molecular mechanics we deal with large molecules whose molecular potential energy is dependent on hundreds or thousands variables (beyond, assessment of the potential energy at each point on the hypersurface is comparatively easy). Optimization methods can be divided into those methods that use derivatives and those that do not use them. Methods using derivatives can be also divided into *first–order* derivative methods (they use gradient) and *second–order* derivative method (use both gradient and Hessian). From many algorithms I will describe three that I make use of. All the algorithms described below are iterative. They start at initial point and then move on in cycles (in accordance with the algorithm) to the stationary point. Each one of the cycles is called an iteration [10].

The first method is a first–order method Steepest descent. The method starts from a point on a molecular potential energy surface and recognizes the fastest way down the surface to the local minimum. This leads into the second point on the potential plane. From this point the next step to another point can be only perpendicular to the first one. This forces every other step to make a right–angle turn at every point even it is not the best way to the minimum. This can also make the algorithm oscillating [10].

The second method also belongs to the first–order methods. It is an algorithm of conjugated gradients. Output of this method is a set of directions that surpass the oscillatory behaviour of steepest descent. Gradual directions are not perpendicular to each other [10].

The third and last method is Quasi–Newton and is included in second–order methods. This method is used when computing Hessian in iteration step is unavailable or too hard to compute. In Quasi–Newton the Hessian matrix does not need to be computed. The Hessian is updated by analysis of successive gradient vectors instead. It restricts the solution by adding an insignificant update to the current estimate of the Hessian [12].

A Gasteiger method was used for calculation of atomic charges of PPy chains and water. It is a rapid calculation of atomic charges in σ–bonded and non–conjugated π–systems. The calculation only considers the connectivity of the atoms because they are characterized by their orbital electronegativities. Therefore, only the topology of a molecule is important. A partial equalization of orbital electronegativity is obtained through an iterative process [13].

The Gasteiger method is inappropriate for calculation of atomic charges of MMT so, in this case was used a charge equilibration method (QEq). It is a great way how to predict charges of large molecules based only on geometry and experimental atomic properties. It also allows the charges to react to changes in the environment (inclusive of those in applied fields) [14].

3. Practical part

3.1 Preparation of composite polypyrrole/montmorillonite

3.1.1 Used materials

Used phyllosilicate for preparation of nanocomposite was montmorillonite (MMT). The crystallochemical formula of this MMT was established at $(Al_{2.56}\ Mg_{0.88}\ Fe^{3+}_{0.56})\ (Si_8)\ O_{20}\ (OH)_4$. Commercially available Na–MMT Portaclay with interlayer distance 1.245 nm and layer charge 0.7 el. was purchased from Ankerpoort, Netherlands. All used chemicals – pyrrole, ferric chloride and ammonium peroxydisulfate – were purchased from Lach–Ner, Czech Republic.

3.1.2 Method of synthesis

Pure PPy powder was prepared by oxidative polymerization of the solution of pyrrole by ammonium peroxydisulfate. Time of the polymerization was 6 hours. The black solid was collected on a filter by rinsing with distilled water and dried for 24 hours at 40°C in a kiln. The same process was used for the second oxidant – ferric chloride.

PPy/MMT composites were prepared using one–step process. The pyrrole and ammonium peroxydisulfate were added into water suspension of MMT. Time of the polymerization was 6 hours. The polymerization mixture was stirred for 6 hours to ensure that the largest possible amount of PPy enters the interlayer space of MMT. The black solid was also collected on a filter by rinsing with distilled water and dried at the same conditions as pure PPy. The composites were also prepared with the second oxidant – ferric chlodride. We also prepared composites with a different amount of pyrrole at the start. Samples with different concentration of pyrrole were prepared by analogical process. There is a sumation of used materials in each sample in Table 1.

Samples were denoted as

N_ P_M_O,

where **N** is number differing the samples, **P** is polypyrrole, **M** is montmorillonite Portaclay, and **O** means type of oxidant (e.g., Fe is ferric chloride and A is ammonium peroxydisulfate). In the beginning we wanted to differ the samples according to the theoretical amount of PPy contained in each sample but then (based on calculations) we found out that the theoretical amount of PPy is actually lower than we thought it is (in percentage units) so we dropped from the naming based on it.

Table 1 *List of samples and used materials.*

Sample	Pyrrole [ml]	MMT [g]	Oxidant [g]
P/A	3.450	–	11.40
10_P_M_A	0.690	4.0	2.28
25_P_M_A	1.725		5.70
50_P_M_A	3.450		11.40
75_P_M_A	5.175		17.10
P/Fe	3.450	–	16.20
10_P_M_Fe	0.690	4.0	3.24
25_P_M_Fe	1.725		8.10
50_P_M_Fe	3.450		16.20
75_P_M_Fe	5.175		24.30

3.2 Analysis of prepared samples

Our samples were analysed by scanning electron microscopy, X–ray powder diffraction, thermogravimetric analysis, Fourier transform infrared spectroscopy and Raman spectroscopy. I also tried to clarify the inner structure of samples by molecular modeling.

Scanning electron microscopy: We studied the morphology of samples on a scanning electron microscope (SEM) Hitachi SU6600 (Hitachi Ltd., Japan). Accelerating voltage was 25 kV. The samples were first dusted with gold and then analyzed with SEM.

Fourier transform infrared spectroscopy: Fourier–transform infrared (FTIR) spectra were recorded in the range of 400 – 4000 cm^{-1}. Samples were measured by ATR technique with diamond crystal on Nicolet 6700 FT–IR (Thermo Scientific, USA) with spectral resolution 0.2 cm^{-1} and 126 scans.

Raman spectroscopy: Raman spectra were collected on Smart System XploRATM (Horiba Jobin Yvon, France) using 532 nm laser source. An Olympus microscope BX 41/51 with an objective magnification of 50 was used to focus the laser beam on the sample placed on an X–Y motorized sample stage. Filter was used to reduce laser beam to 1% of initial laser beam and grating 1800 grooves/mm were used. Acquisition time was set to the 30 s.

Thermogravimetric analysis: Simultaneous thermogravimeter–differential scanning calorimeter (TG–DSC) STA 409 EP (Netzsch) equipped with a high–sensitive analytical balance was used for measuring the mass change of the samples (10^1 mg in weight) as a function of time or temperature. All samples were heated up to 1000 °C, with heatign rate 10 °C·min^{-1}, in the crucibles (α–Al_2O_3) in a dynamic atmosphere of dry air with a flow rate of 100 cm^3·min^{-1}.

X–ray powder diffraction: The X–ray diffraction patterns were recorded using Bruker D8 Advance diffractometer (Bruker AXS, Germany) equipped with fast position sensitive detector VÅNTEC 1. CoK_α irradiation (λ = 0.1789 nm) was used. Measurements of all samples were carried out in reflection mode in symmetrical Bragg–Brentano arrangement.

Molecular modeling: Models were prepared in BIOVIA Materials studio v0.7 (Accelrys) according to data from the thermogravimetric analysis (weight loss of organic compound and water) and X–ray diffraction. I prepared two kind of models according to the dependence of amount of PPy and weight percent (wt.%) of water whose influence the interlayer spacing. Both kinds of models contained modeled structure of MMT–Portaclay ($(Al_{2.85}Mg_{0.71}Fe^{3+}_{0.42})Si_8O_{20}(OH)_4$), prepared as a periodic structure; sodium cations, molecules of water and chains of PPy (modeled

with 10 rings) with different charge (polarons and bipolarons) but not their combination. Charge on the MMT structure was calculated by QEq method and charges for PPy and water were calculated by Gasteiger method. Models containing 2 – 6 polarons were modeled with 0.5, 1.0, 1.5, 4.0, and 6.0 wt.% of water. Model with one polaron was modeled with 1.0, 4.0, and 6.0 wt.% of water. Model with 2 and 3 bipolarons were modeled with 0.5, 1.0, 1.5, 4.0, and 6.0 wt.% of water. Model with one bipolaron was modeled with 1.0, 4.0, and 6.0 wt.% of water. There were always three models of each type with different inner arrangement of molecules. After building, the models were optimized by module Forcite in mode smart (using three algorithms: Steepest descent, Conjugated gradients and Quasi–Newton), maximum amount of iterations was set to $5 \cdot 10^5$ and pressure was set to 101 325 Pa. The calculation was done when potential energy has reached the accuracy of 0.001 kcal/mol and the force reached accuracy 0.5 kcal/mol/Å. From each trinity of models was chosen the model with the lowest potential energy. These models were then analyzed by Reflex modul that was set according to the real measurements of X–ray diffraction (λ = 1.7889 Å, Bragg–Brentano arrangement). Calculated interlayer distances were then evaluated in form of a graph where the interlayer distance depends on the water and PPy content. In the graph were also included measured interlayer distances (X–ray diffraction) and wt.% of water (thermogravimetric analysis) of real samples (four graphs – polaron and bipolaron both prepared using different oxidant).

3.3 Results

3.3.1 Results of analysis

Scanning electron microscopy: The following pictures show the morphology of pure PPy prepared with two different oxidants and composites with 50 percent amount of pyrrole in base (also using two oxidants as in case of pure PPy). There are PPy and composite prepared using ferric chloride in Fig. 12 and Fig. 13. There are PPy and composite prepared using peroxydisulfate in Fig. 14 and Fig. 15. It is obvious that prepared pure PPy forms ball–shaped grains in both cases (both oxidants). There are particles covered with PPy chains (Fig. 13 and Fig. 15). The particles are fully covered – there is not any appearance of uncovered spots. This means that the prepared nanocomposite material is to some extent homogenous. The polymer is presented both on the surface and inside the interlayer space.

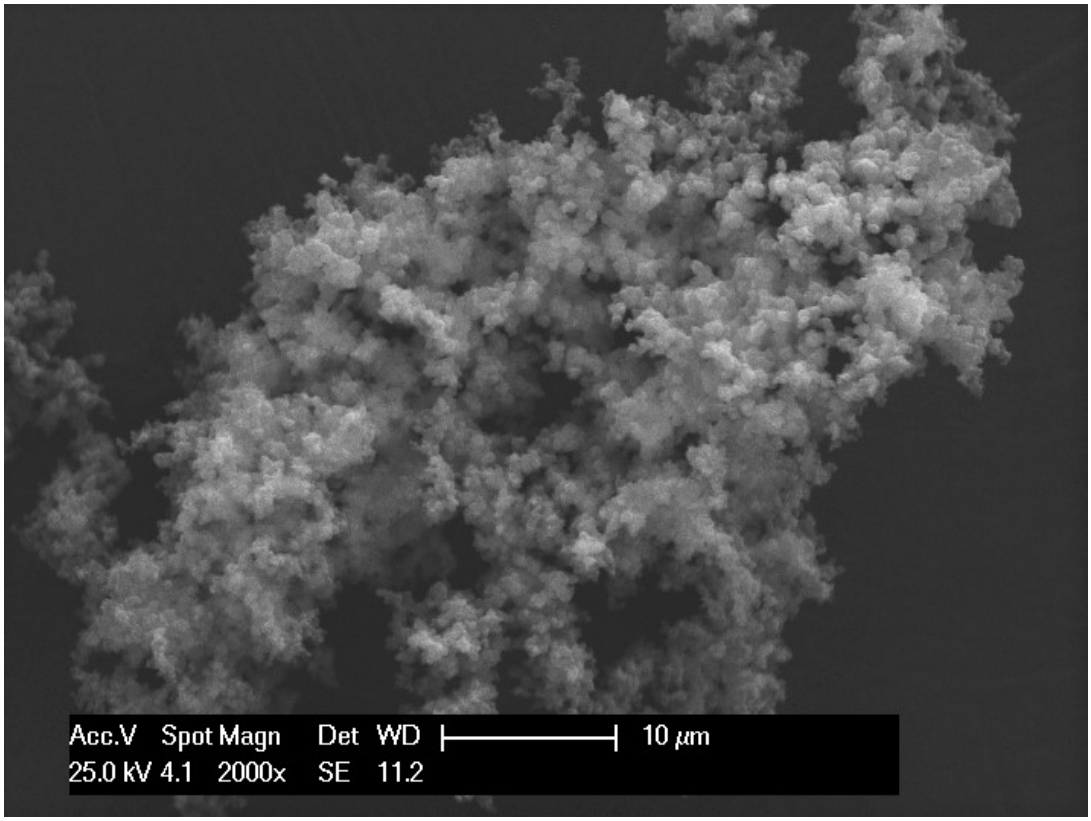

Fig. 12 *Pure polypyrrole prepared using ferric chloride (sample P/Fe).*

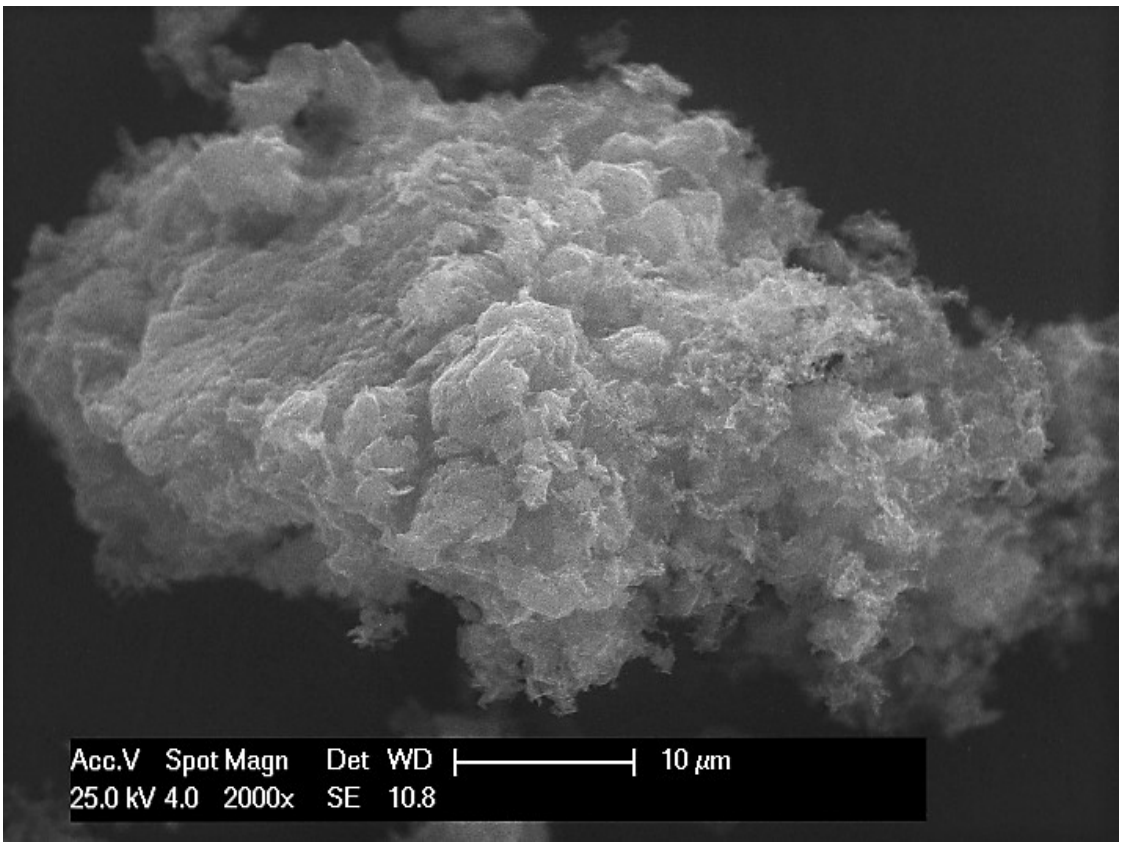

Fig. 13 *Nanocomposite polypyrrole/montmorillonite prepared using ferric chloride (sample 50_P_M_Fe).*

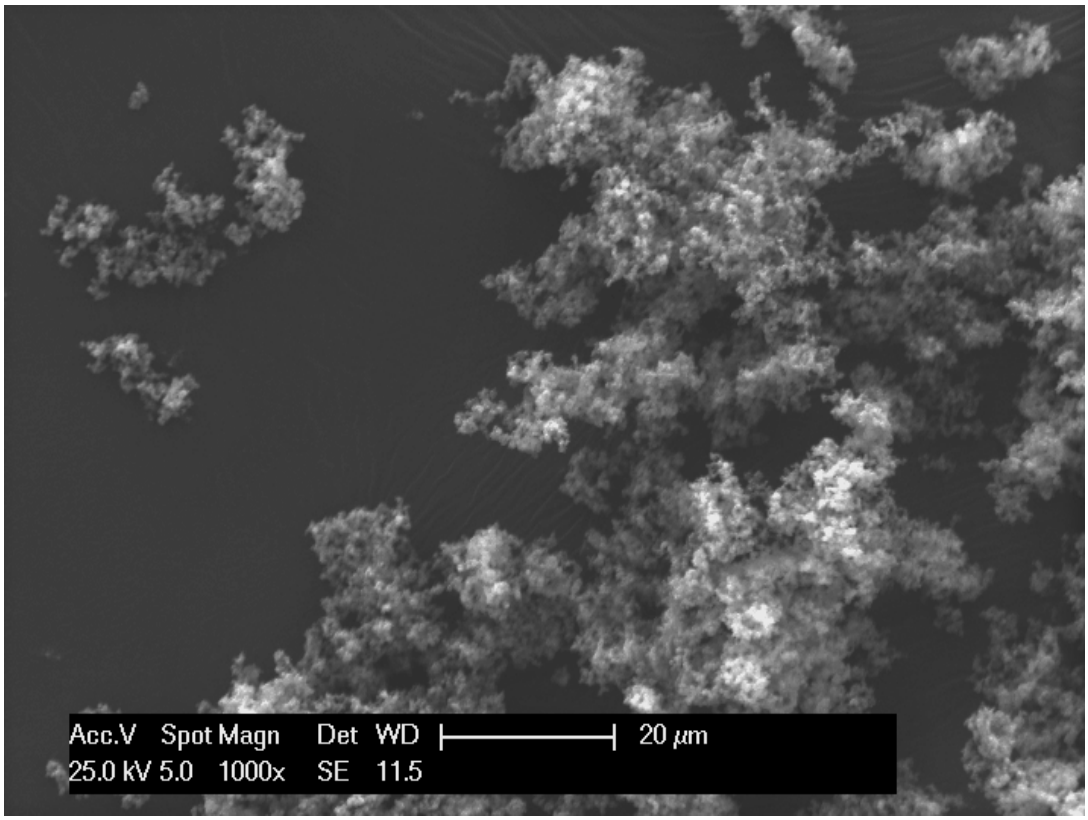

Fig. 14 *Pure polypyrrole prepared using peroxydisulfate (sample P/A).*

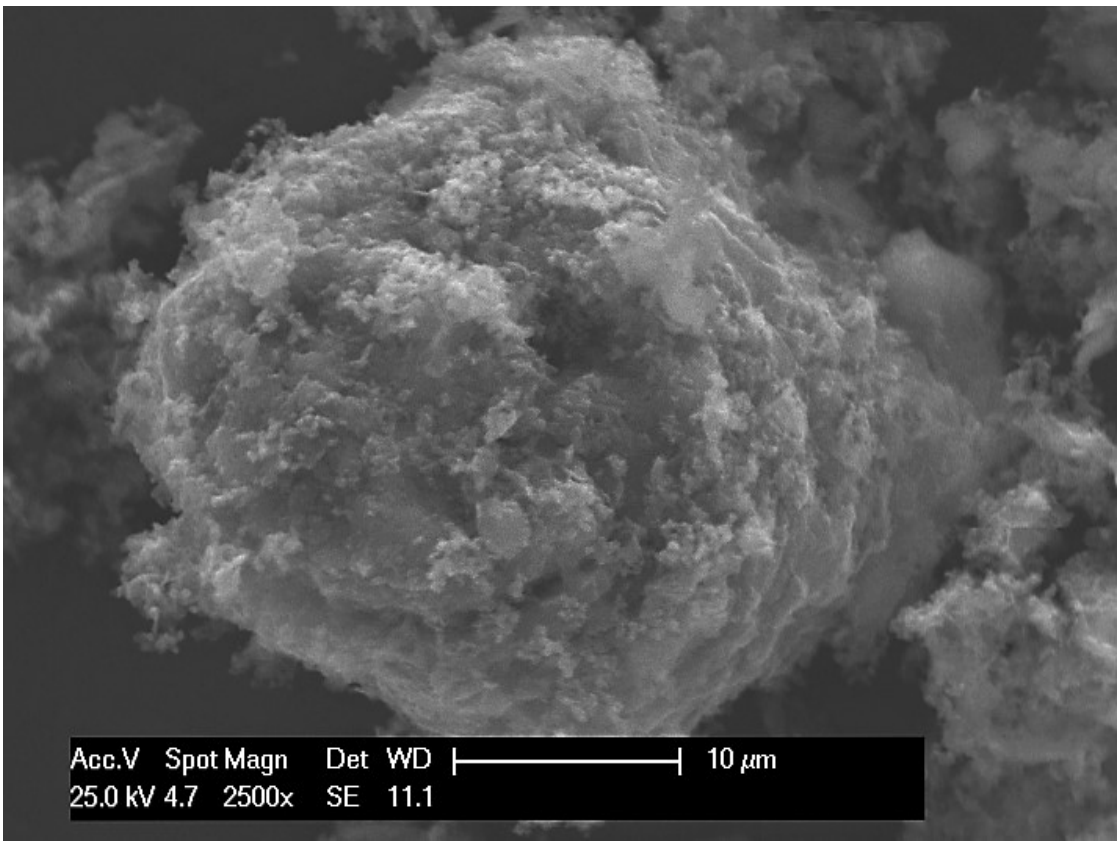

Fig. 15 *Nanocomposite polypyrrole/montmorillonite prepared using peroxydisulfate (sample 50_P_M_A).*

Infrared spectroscopy: Measured infrared spectra of samples 50_P_M_A, 50_P_M_Fe, P/A, and P/Fe are shown in Fig. 16. Determination of the all characteristic bands of PPy is not clear and it is difficult to find the references for interpretation of the measured spectra. Although main bands could be described as follows: stretching vibration of C=C/C–C of PPy chains (1540 cm^{-1}), vibration of C=N (1453 cm^{-1}), and deformation vibration of C–H/N–H (1292 cm^{-1}). These bands position correspond to the samples 50_P_M_A and P/A. Bands position of the samples 50_P_M_Fe and P/Fe are shifted to the lower wavenumbers (1521, 1436, and 1278 cm^{-1}) which could be explained by presence of a longer "delocalized length" of the polyconjugated system [15]. Shoulder at 870 cm^{-1}, which is marked with arrow in the Fig. 16 is considered to be associated with conductivity and its decrease intensity is connected with loss conductivity, according this statement less conductive samples probably could be samples 50_P_M_A and P/A [16].

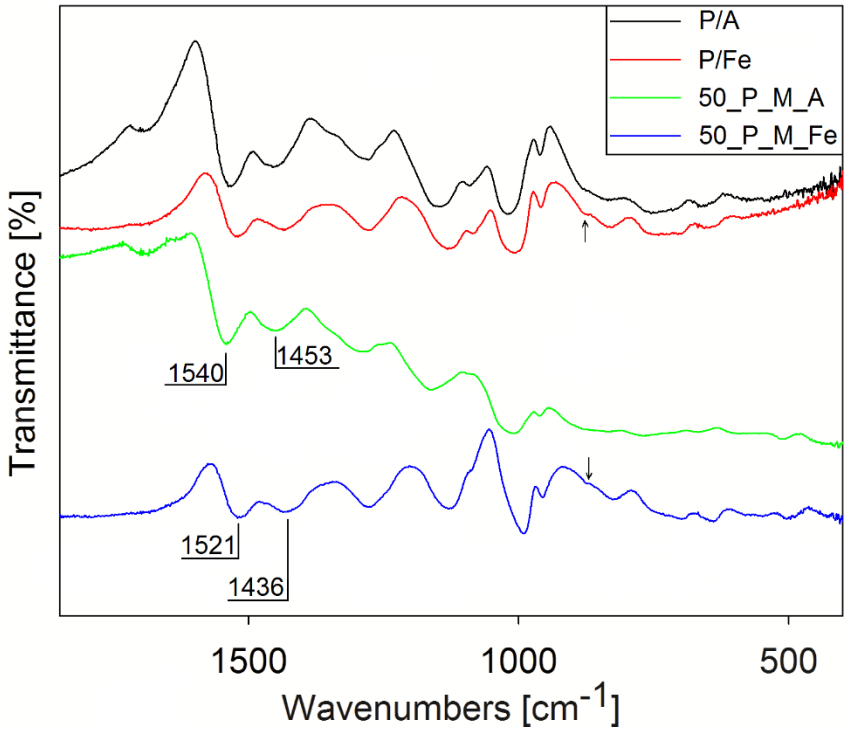

Fig. 16 *Infrared spectra of pure polypyrrole (P/A, P/Fe) and nanocomposites (50_P_M_A, 50_P_M_Fe).*

Raman spectroscopy: Measured Raman spectra of samples P/A, P/Fe, 50_P_M_A, and 50_P_M_Fe are shown in Fig. 17. Band about 1585 cm^{-1} represents the C=C backbone stretching of PPy chains and its position is related to the sample conductivity (lower wavenumbers of the band should mean better conductivity). The band located at 1060 cm^{-1} is classified as C–H in–plane deformation vibrations of oxidized PPy [17]. The band at 1328 cm^{-1} is associated with ring stretching vibrations, and two peaks at 976 and 936 cm^{-1} correspond to ring deformation vibrations connected with cation radical (polaron) and dication diradical (bipolaron) structures of PPy [18].

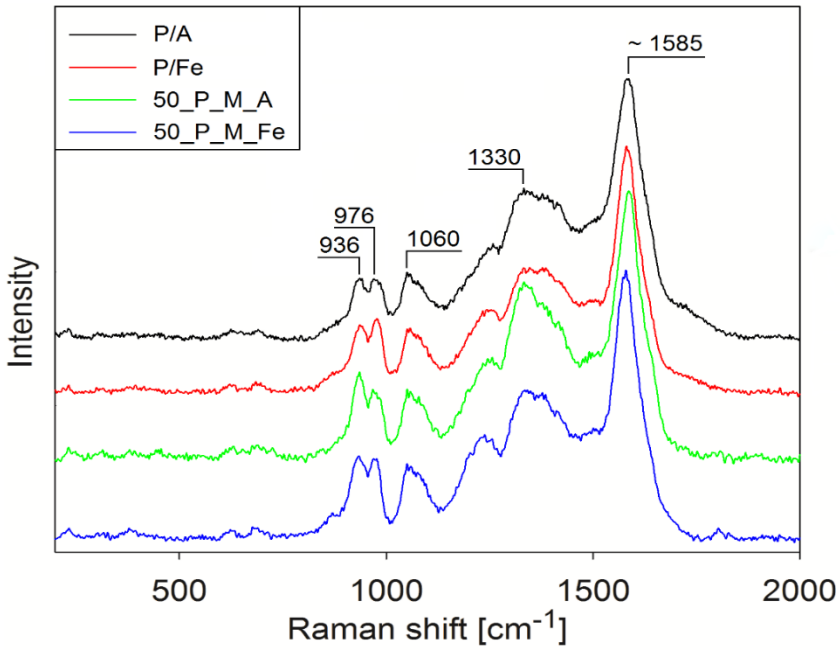

Fig. 17 *Raman spectra of pure polypyrrole (P/A, P/Fe) and nanocomposites (50_P_M_A, 50_P_M_Fe).*

Thermogravimetric analysis: In Table 2 are gathered weight losses of all samples with increasing temperature. Values Δm_1 represent weight loss of surface water (up to 110°C), Δm_2 is a weight loss of interlayer water and organic compound (110 – 200 °C), Δm_3 is a weight loss of organic compound (200 – 580 °C), Δm_4 is a weight loss constitutional water and organic compound (580 – 800 °C).

Table 2 *Results of thermogravimetric analysis due to change of temperature.*

Sample	Δm_1 [%]	Δm_2 [%]	Δm_3 [%]	Δm_4 [%]
10_P_M_A	2.2	0.6	12.2	3.8
25_P_M_A	2.5	1.6	24.5	5.7
50_P_M_A	3.3	1.0	35.2	5.9
75_P_M_A	2.6	1.3	45.7	7.7
10_P_M_Fe	2.9	1.7	7.7	7.4
25_P_M_Fe	2.6	2.1	19.8	9.7
50_P_M_Fe	2.1	1.6	38.3	8.9
75_P_M_Fe	3.1	1.5	44.9	3.2
MMT–Portaclay	3.8	1.0	–	3.0

X–ray powder diffraction: Fig. 18 shows diffraction pattern for samples prepared with $FeCl_3$ (each colour for a different sample). There are two major peaks for sample 10_P_M_Fe that were both taken for further analysis. From peak of the sample 25_P_M_Fe can be told that this sample has the most ordered structure – homogeneous intercalation (a great representation of similar interlayer distances). This structure is then more and more broken, for higher amount of PPy presented in sample (50_P_M_Fe and 75_P_M_Fe) and intensity of peaks decreases (the lowest value for sample 75_P_M_Fe). From the shift (to the left) of all peaks instead of the peak of pure MMT can be assumed the interlayer space of all samples has been magnified. In Table 3 there are summarized the interlayer distances and the full widths at half maximum (FWHM) for samples prepared using ferric chloride as an oxidant. In Fig. **19** is shown diffraction pattern for samples prepared with ammonium peroxydisulfate. The shift (to the right) for the peaks of samples 10_P_M_A and 25_P_M_A indicates reduction of the interlayer space of mentioned samples. This can be caused by decrease of water content in the interlayer space. Even that the interlayer distance was decreased, we cannot say the intercalation didn't happen. The peaks for samples 50_P_M_A and 75_P_M_A indicate that their intercalation is homogenous and the interlayer distance increased in both cases. Table 4 summarizes the interlayer distances and the full widths at half maximum for samples prepared using peroxydisulfate as an oxidant. The most intercalated sample was 25_P_M_Fe according to the interlayer distance 17.631 Å (Table 3). Higher concentration of ferric chloride in sample contributes to breakage of the composite structure (according to comparison of diffraction patterns for both oxidants.

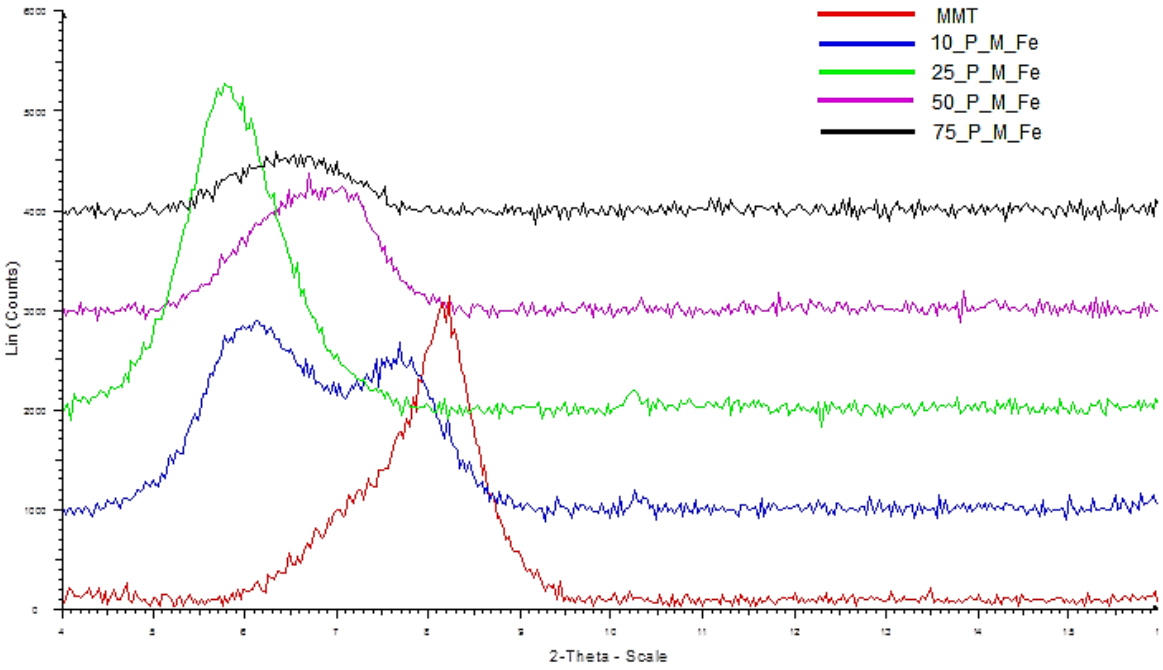

Fig. 18 *Diffraction pattern for samples prepared using ferric chloride as an oxidant.*

Table 3 *List of interlayer distances (d) and full widths at half maximum (FWHM) for samples prepared using ferric chloride as an oxidant.*

Sample	d [Å]	FWHM [°]
MMT–Portaclay	12.569	0.938
10_P_M_Fe – left peak	17.176	0.988
10_P_M_Fe – right peak	13.344	0.623
25_P_M_Fe	17.631	1.169
50_P_M_Fe	15.315	1.498
75_P_M_Fe	16.192	1.550

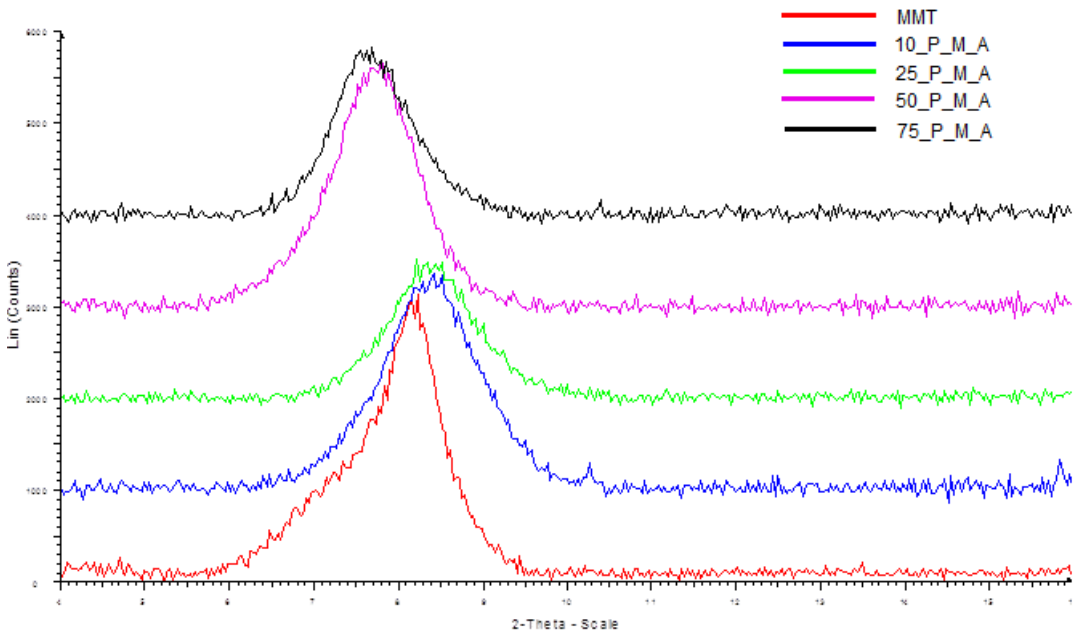

Fig. 19 *Diffraction pattern for samples prepared using peroxydisulfate as an oxidant.*

Table 4 *List of interlayer distances (d) and full widths at half maximum (FWHM) for samples prepared using peroxydisulfate as an oxidant.*

Sample	d [Å]	FWHM [°]
MMT–Portaclay	12.569	0.938
10_P_M_A	12.262	1.247
25_P_M_A	12.488	1.173
50_P_M_A	13.274	1.175
75_P_M_A	13.404	1.042

3.3.2 Results of molecular modeling

Graphs in Figs. 20 – 23 correspond to optimized models containing polaron and bipolaron PPy chains both for each oxidant, ferric chloride (Figs. 20 and 21) and ammonium peroxydisulfate (Figs. 22 and 23). Fig. 20 and Fig. 21 suggest that the sample 10_P_M_Fe can be assigned to the model with 1.5 wt.% of water and five or six molecules of PPy polaron (according to the diffraction pattern of the real sample – left peak) The model with six molecules of PPy is more presumable due to the intersection of the interlayer distance value with curve of models with 6 PPy in lower

amount of water. To the value of the right peak of the real sample can be assigned the model with 1.5 wt.% of water and two or three molecules of PPy polaron or three molecules of PPy bipolaron. The sample 25_P_M_Fe can be classified by the model with 2.0 wt.% of water and 6 molecules of PPy polaron. This was only deduced from the graph because we did not model the models with 2.0 wt.% of water. The sample 50_P_M_Fe can be assigned to the model with 1.5 wt.% of water and four or five molecules of PPy polaron. The model with 1.0 wt.% of water and five molecules of PPy polaron corresponds with the real sample 75_P_M_Fe. According to the data form Fig. 21 may be said that the bipolaron structure of PPy mostly does not occur in the samples prepared using ferric chloride as an oxidant.

The Fig. 22 and Fig. 23 were evaluated for the samples prepared using peroxydisulfate as an oxidant. From the data it can be said that both polaron and bipolarons structures occur in prepared samples. The real sample 10_P_M_A can be classified by the models with 0.5 wt.% of water and two molecules of PPy polaron or two to three molecules of PPy bipolaron (it cannot be said whether there are two or three molecules because the interlayer distance value does not intersect any curve in lower amount of water). The sample 25_P_M_A can be assigned to the models with 1.5 wt.% of water and two molecules of PPy polaron or two molecules of PPy bipolaron. The models with 0.5 wt.% of water and three molecules of PPy polaron or three molecules PPy bipolaron can be allocated to the sample 50_P_M_A. The models with 1.0 wt.% of water and three molecules of PPy polaron and three molecules of PPy bipolaron matches the sample 75_P_M_A. All the models that were assigned to the real samples and mentioned above are listed in Attachment A.

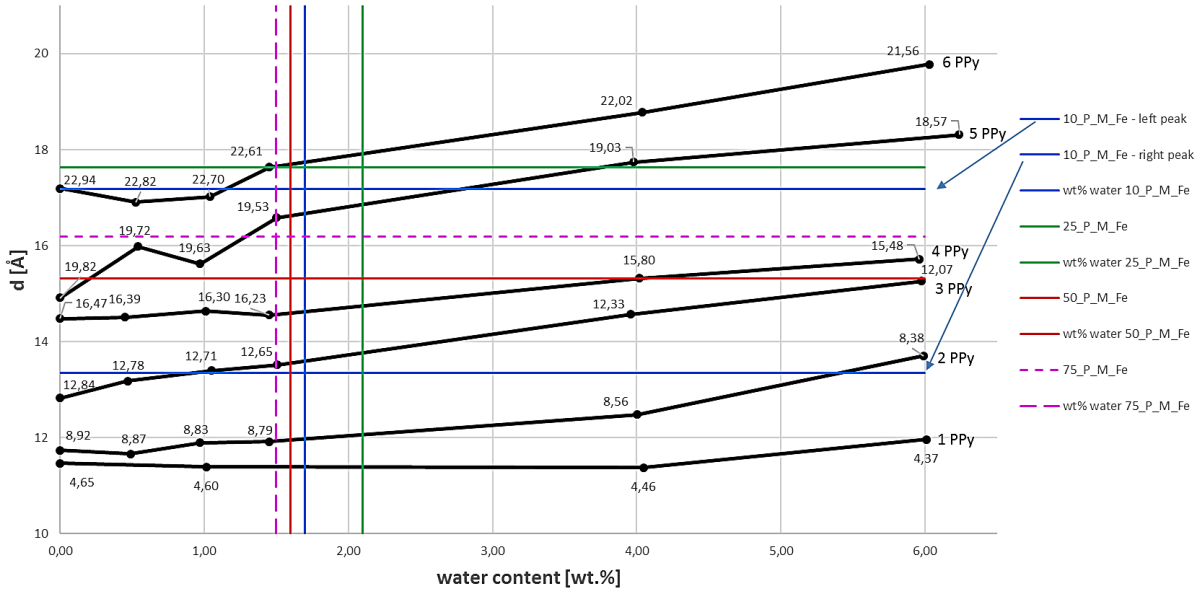

Fig. 20 *Basal spacing (d) and amounts of interlayer content obtained from models containing PPy molecules (polaron). Comparison with data of samples prepared using ferric chloride.*

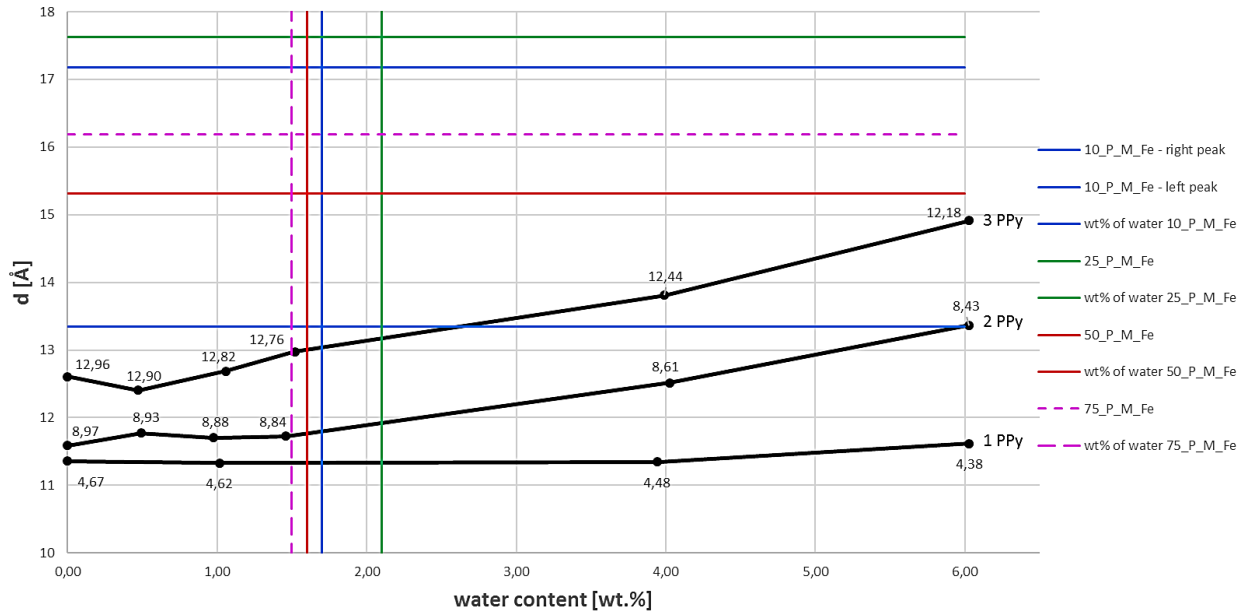

Fig. 21 *Basal spacing (d) and amounts of interlayer content obtained from models containing PPy molecules (bipolaron). Comparison with data of samples prepared using ferric chloride.*

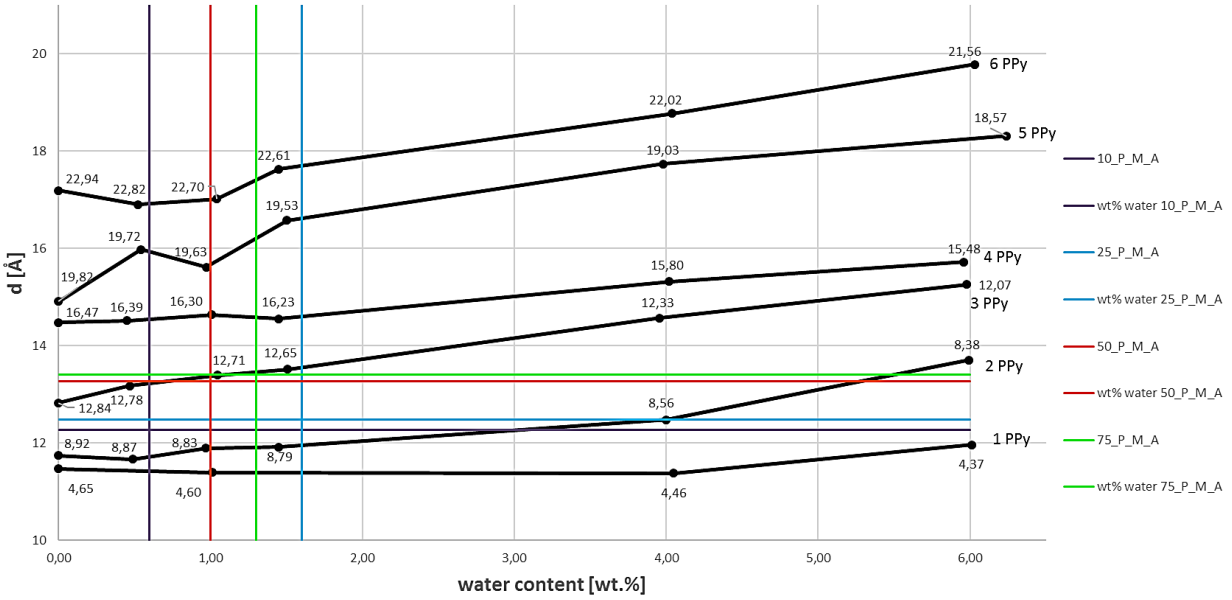

Fig. 22 *Basal spacing (d) and amounts of interlayer content obtained from models containing PPy molecules (polaron). Comparison with data of samples prepared using peroxydisulfate.*

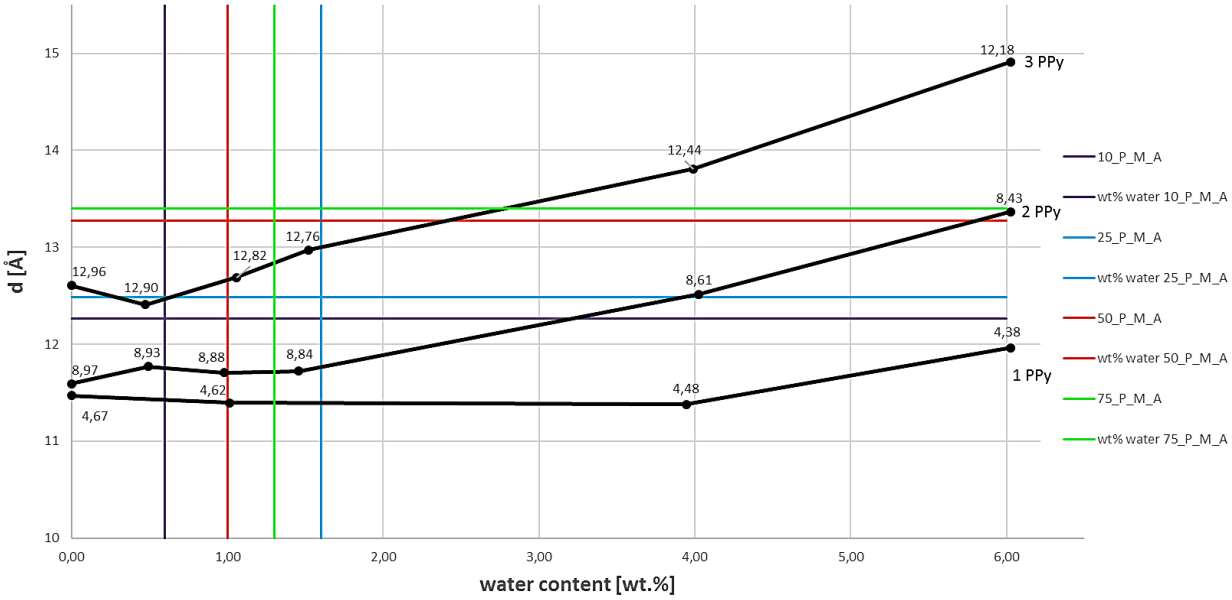

Fig. 23 *Basal spacing (d) and amounts of interlayer content obtained from models containing PPy molecules (bipolaron). Comparison with data of samples prepared using peroxydisulfate.*

4. Conclusion

In my work I successfully prepared nanocomposites of polypyrrole/phyllosilicate type with two oxidizing agents. Prepared samples were analysed by X–ray diffraction, which for the samples prepared using ferric chloride confirmed expansion of interlayer space, indicating intercalation of the polymer into it. Two separated peaks can be found in the X-ray diffraction pattern of the sample 10_P_M_Fe. This fact indicates the presence of strongly heterogeneous structure. In further analysis, I have compiled a series of molecular models that indicate possible internal arrangement of the prepared samples. The sample 10_P_M_Fe (left peak) corresponds with model containing 1.5 wt.% of water and 19.53 – 22.61 wt.% of PPy polaron, for the right peak it is model containing 1.5 wt.% of water and 8.79 – 12.65 wt.% of PPy polaron or 12.76 wt.% of PPy bipolaron. The sample 25_P_M_Fe does not correspond with any prepared model but according to the data we can suppose that it would correspond with model containing 2.0 wt.% of water and 22.49 wt.% of PPy polaron. The sample 50_P_M_Fe agrees with model containing 1.5 wt.% of water and 16.23 – 19.53 wt.% of PPy polaron. The sample 75_P_M_Fe corresponds with model containing 1.0 wt.% of water and 19.63 wt.% of PPy polaron. The sample 10_P_M_A matches with model containing 0.5 wt.% of water and 8.87 wt.% of PPy polaron or 8.93 – 12.90 wt.% of PPy bipolaron. The sample 25_P_M_A correspond with model containing 1.5 wt.% of water and 8.79 wt.% of PPy polaron or 8.84 wt.% of PPy bipolaron. The sample 50_P_M_A agrees with model containing 0.5 wt.% of water and 12.78 wt.% of PPy polaron or 12.90 wt.% of PPy bipolaron. The sample 75_P_M_A corresponds with model containing 1.0 wt.% of water and 12.71 wt.% of PPy polaron or 12.82 wt.% of PPy bipolaron. The models give a general idea of how the interlayer space looks like. Unfortunately, my work does not include an analysis of the electrical conductivity of nanocomposites prepared. However, this issue is great for analysis in a subsequent study.

Literature

[1] GOTTWALD, Tomáš. Vodivé polymery a jejich využití v superkondenzátorech: Conducting polymers and their use in supercapacitors [CD-ROM]. Brno: Vysoké učení technické, Fakulta elektrotechniky a komunikačních technologií, 2010. 57s Diplomová práce.

[2] PROKEŠ, Jan, Jaroslav STEJSKAL a Mária OMASTOVÁ. Polyanilin a polypyrrol - dva představitelé vodivých polymerů. Chemické listy. 2001, 95(8), 484-492.

[3] PRATESI, Pietro, Sui neri di pirrolo, *Gazzett Chimica Italiana*, 67, 188 (1937)

[4] VERNITSKAYA, Tat'yana V a Oleg N EFIMOV. Polypyrrole: a conducting polymer; its synthesis, properties and applications. *Russian Chemical Reviews* [online]. 1997, 66(5), 443-457 [cit. 2016-04-28]. DOI: 10.1070/RC1997v066n05ABEH000261. ISSN 0036021x.

[5] VALÁŠKOVÁ, Marta. *Vybrané vrstevnaté silikáty a jejich modifikované nanomateriály*. Vyd. 1. Brno: Akademické nakladatelství CERM, 2012, 148 s. ISBN 978-80-7204-811-3.

[6] MELKA, Karel a Martin ŠŤASTNÝ. Encyklopedický přehled jílových a příbuzných minerálů. 1. vyd. Praha: Academia, 2014. Neživá příroda. ISBN 9788020023698.

[7] VOLZONE, C., J. O. RINALDI a J. ORTIGA. N_2 and CO_2 Adsorption by TMA- and HDP-Montmorillonites. *Materials Research* [online]. 2002, 5(4), 475-479, DOI: 10.1590/S1516-14392002000400013. ISSN 1516-1439.

[8] ALEXANDRE, Michael a Philippe DUBOIS. Polymer-layered silicate nanocomposites: preparation, properties and uses of a new class of materials. Materials Science and Engineering: R: Reports [online]. 2000, 28(1-2), 1-63 [cit. 2016-04-27]. DOI: 10.1016/S0927-796X(00)00012-7. ISSN 0927796x.

[9] Dostupné z: http://linkinghub.elsevier.com/retrieve/pii/S0927796X00000127

[10] KIM, J.W, F LIU, H.J CHOI, S.H HONG a J JOO. Intercalated polypyrrole/Na^+-montmorillonite nanocomposite via an inverted emulsion pathway method. Polymer [online]. 2003, 44(1), 289-293 [cit. 2016-04-27]. DOI: 10.1016/S0032-3861(02)00749-8. ISSN 00323861.
Dostupné z: http://linkinghub.elsevier.com/retrieve/pii/S0032386102007498

[11] HINCHLIFFE, Alan. *Molecular modelling for beginners*. 2nd ed. Hoboken, NJ: Wiley, 2008. ISBN 0470513144.

[12] RAPPE, A. K., C. J. CASEWIT, K. S. COLWELL, W. A. GODDARD a W. M. SKIFF. UFF, a full periodic table force field for molecular mechanics and molecular dynamics simulations. Journal of the American Chemical Society [online]. 1992, 114(25), 10024-10035 [cit. 2016-05-01]. DOI: 10.1021/ja00051a040. ISSN 00027863.
Dostupné z: http://pubs.acs.org/doi/abs/10.1021/ja00051a040

[13] SCHOENBERG, Ronald. *Optimization with the Quasi-Newton Method* [online]. 2001, 13 [cit. 2016-05-01]. Dostupné z: http://www.aptech.com/wp-content/uploads/2013/05/qnewton.pdf

[14] GASTEIGER, Johann a Mario MARSILI. Iterative partial equalization of orbital electronegativity—a rapid access to atomic charges. Tetrahedron [online]. 1980, 36(22), 3219-3228 [cit. 2016-05-01]. DOI: 10.1016/0040-4020(80)80168-2. ISSN 00404020.
Dostupné z: http://linkinghub.elsevier.com/retrieve/pii/0040402080801682

[15] RAPPE, Anthony K. a William A. GODDARD. Charge equilibration for molecular dynamics simulations. The Journal of Physical Chemistry [online]. 1991, 95(8), 3358-3363 [cit. 2016-05-01]. DOI: 10.1021/j100161a070. ISSN 00223654. Dostupné z: http://pubs.acs.org/doi/abs/10.1021/j100161a070

[16] TABAČIAROVÁ, Jana, Matej MIČUŠÍK, Pavol FEDORKO a Mária OMASTOVÁ. Study of polypyrrole aging by XPS, FTIR and conductivity measurements. Polymer Degradation and Stability [online]. 2015, 120, 392-401 [cit. 2016-05-01]. DOI: 10.1016/j.polymdegradstab.2015.07.021. ISSN 01413910.
Dostupné z: http://linkinghub.elsevier.com/retrieve/pii/S0141391015300537 4

[17] MATHYS, G.I. a V.T. TRUONG. Spectroscopic study of thermo-oxidative degradation of polypyrrole powder by FT-IR. Synthetic Metals [online]. 1997, 89(2), 103-109 [cit. 2016-05-01]. DOI: 10.1016/S0379-6779(98)80122-7. ISSN 03796779.
Dostupné z: http://linkinghub.elsevier.com/retrieve/pii/S0379677998801227

[18] CHEN, Wei, Chang Ming LI, Peng CHEN a C.Q. SUN. Electrosynthesis and characterization of polypyrrole/Au nanocomposite. Electrochimica Acta [online]. 2007, 52(8), 2845-2849 [cit. 2016-05-01]. DOI: 10.1016/j.electacta.2006.07.005. ISSN 00134686.
Dostupné z: http://linkinghub.elsevier.com/retrieve/pii/S0013468606007183

[19] OMASTOVÁ, Mária, Katarína MOSNÁČKOVÁ, Pavol FEDORKO, Miroslava TRCHOVÁ a Jaroslav STEJSKAL. Polypyrrole/silver composites prepared by single-step synthesis. Synthetic Metals [online]. 2013, 166, 57-62 [cit. 2016-05-01]. DOI: 10.1016/j.synthmet.2013.01.015. ISSN 03796779. Dostupné z: http://linkinghub.elsevier.com/retrieve/pii/S0379677913000416

Acknowledgements

First and foremost, I would like to thank Assoc. Prof. Ing. Lenka Kulhánková, Ph.D., and Assoc. Prof. Ing. Jonáš Tokarský, Ph.D., for their responsible and professional guidance, help and the trust they put in me. I hope they were satisfied with my work. I would also like to thank Mgr. Kateřina Mamulová Kutláková, Ph.D., for the performance and evaluation of X-ray diffraction analysis, to Mrs. Marie Heliová for scanning electron microscopy, to Ing. Silvie Vallová, Ph.D., for thermogravimetric analysis, and Mgr. Pavlína Peikertová, Ph.D., for Fourier transform infrared and Raman spectroscopy. Research described in this bachelor thesis has been supported by the Ministry of Education, Youth and Sports of the Czech Republic (project reg. no. SP2016/63) and the NPU II – IT4Innovations excellence in science (project reg. no. LQ1602).